

Mechanical behaviour of the lithosphere beneath the Adamawa Uplift (Cameroon, West Africa) based on gravity data

Y. H. POUDJOM DJOMANI, M. DIAMENT* and Y. ALBOUY**

Université de Paris Sud, Lab. de Géophysique (URA 1369 du CNRS), Bat. 509, 91405 Orsay Cédex France

*IPG Paris, Département des Observatoires, 4 place Jussieu, B89, 75252 Paris Cedex 05, France

**ORSTOM, Lab. de Géophysique, 72 route d'Aulnay, 93140 Bondy, France

(First received 25th September, 1991; revised form received 27th April, 1992)

Abstract - The Adamawa massif in Central Cameroon is one of the African domal uplifts of volcanic origin. It is an elongated feature, 200 km wide.

The gravity anomalies over the Adamawa uplift were studied to determine the mechanical behaviour of the lithosphere. Two approaches were used to analyse six gravity profiles that are 600 km long and that run perpendicular to the Adamawa trend. Firstly, the coherence function between topography and gravity was interpreted; secondly, source depth estimations by spectral analysis of the gravity data was performed. To get significant information for the interpretation of the experimental coherence function, the length of the profiles was varied from 320 km to 600 km. This treatment allows one to obtain numerical estimates of the coherence function.

The coherence function analysis points out that the lithosphere is deflected and thin beneath the Adamawa uplift, and the Effective Elastic Thickness is of about 20 km. To fit the coherence, a load from below needs to be taken into account. This result on the Adamawa massif is of the same order of magnitude as those obtained on other African uplifts such as Hoggar, Darfur and Kenya domes.

For the depth estimation, three major density contrasts were found: the shallowest depth (4-15 km) can be correlated to shear zone structures and the associated sedimentary basins beneath the uplift; the second density contrast (18-38 km) corresponds to the Moho; and finally, the last depth (70-90 km) would be the top of the upper mantle and denotes the low density zone beneath the Adamawa uplift.

INTRODUCTION

The Adamawa uplift in Central Cameroon is a volcanic dome which was formed during Tertiary times together with other African uplifts: Darfur, Hoggar, Tibesti, Air (Fig. 1). The Adamawa plateau is located at the northeastern limit of the "Cameroon volcanic line" which comprises a series of Tertiary to Recent volcanoes from the Atlantic island of Annobon to the Bambouto and Oku mountains in Cameroon. This volcanic line splits into two branches at the north of Oku: one branch crossing the Benue trough into eastern Nigeria (Biu plateau), and the other branch running eastward to the Adamawa plateau (Fig. 2). The Adamawa uplift is an elongated feature of 200 km wide. The origin of the volcanism on the Cameroon line is still a matter of discussion; for the continental part of the line, 1) it has been proposed that this volcanism was associated with intracontinental hotspots (Fitton, 1980, 1983; Tchoua, 1974; Duncan, 1981); 2) the volcanism could be related to a rejuvenation of major faults that either exist before the opening of the South Atlantic Ocean or are related to an early stage of the seafloor spreading (Vincent, 1970; Mascle, 1976;

Cornacchia et Dars, 1983; Reyre, 1984; Almeida et Black, 1967; Louis, 1970, 1978). The active volcano on the Cameroon line is Mount Cameroon where the last eruption occurred in 1982.

A Bouguer anomaly map of Cameroon, computed from ORSTOM data shows that the Adamawa massif is characterized by a long wavelength negative Bouguer anomaly of about -120 mgals (Collignon, 1968). Seismological studies (C. and L. Dorbath, 1984) revealed the presence of an abnormal upper mantle beneath the Adamawa uplift.

In this study, we interpret the gravity data: in order first to determine the mechanical behaviour of the lithosphere by estimating the flexural rigidity and thus the Effective Elastic Thickness of the lithosphere beneath the Adamawa uplift. The approach used in this first part is the analysis of the coherence function between the gravity and the topography. The results are compared to those obtained on the other African domes and some continental rift areas using the same approach. Finally, we perform source depth estimations by a spectral analysis of the gravity data to find the depth of the major density contrasts.

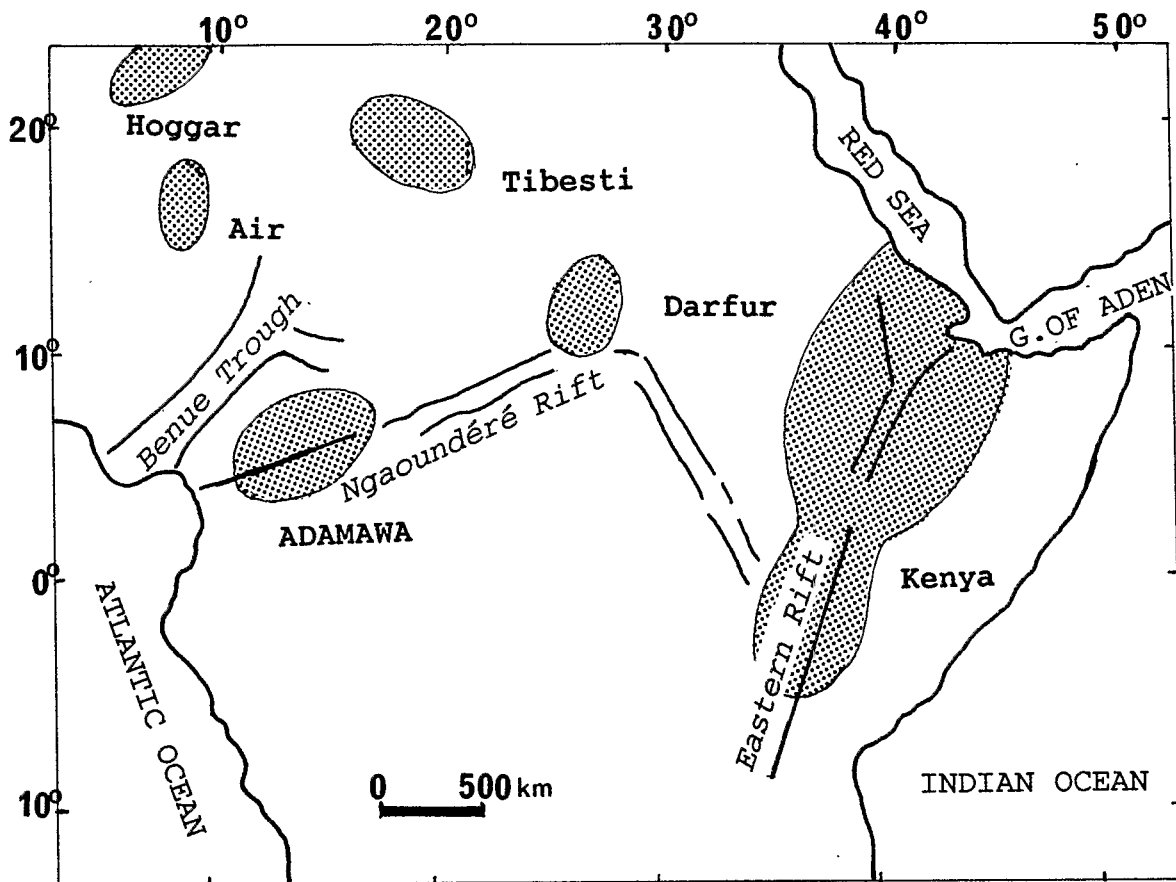


Fig. 1. Location of volcanic domes in Northern and Central Africa (redrawn from Browne and Fairhead, 1983).

ADAMAWA: GEODYNAMICAL CONTEXT

Central Cameroon in Central Africa has been affected by the Pan-African cycle (600 ± 100 Ma) which produced deformation, metamorphism and intrusion of abundant granitoids. During the stages of the Pan-African, important tectonic movements occurred by megashear zones orientated ENE-WSW from Sudan to Cameroon (Cornacchia and Dars, 1983).

During the initial phases of the opening of the south Atlantic ocean (Cretaceous) a series of subsiding grabens and troughs filled in by sediments were formed: Benue in Nigeria-Cameroon, Doba, Bouso in Chad, Mbere-Djerem in south Adamawa. Some rifts were also initiated (Ngaoundere, Abu Gabra and others).

A reactivation of the Ngaoundere rift occurred during Tertiary times, and so was the formation of some African volcanic domes as Adamawa, Darfur, Air, Hoggar... (Browne and Fairhead, 1983) (see Fig. 1). The Adamawa massif represents a post-Cretaceous uplifted area at the north-eastern limit of the Cameroon volcanic line.

Some geophysical studies have been carried out on this domal uplift:

- Collignon (1968) showed that Adamawa is characterized by a long wavelength negative

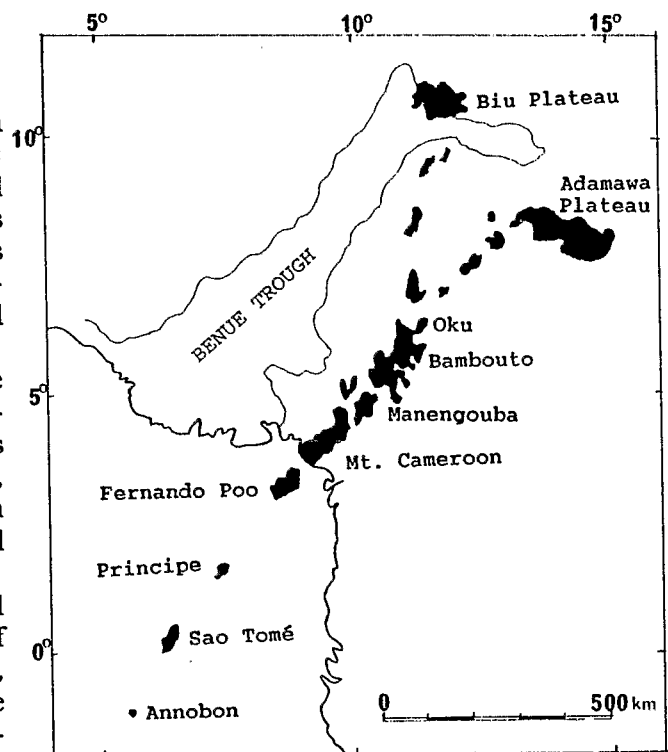


Fig. 2. Position of the Cameroon volcanic line in Africa. Bouguer anomaly, of about -120 mgals and 200 km wide (Fig. 3). Following Browne and Fairhead's interpretation (1983), this anomaly is due to a low density body in the upper mantle.

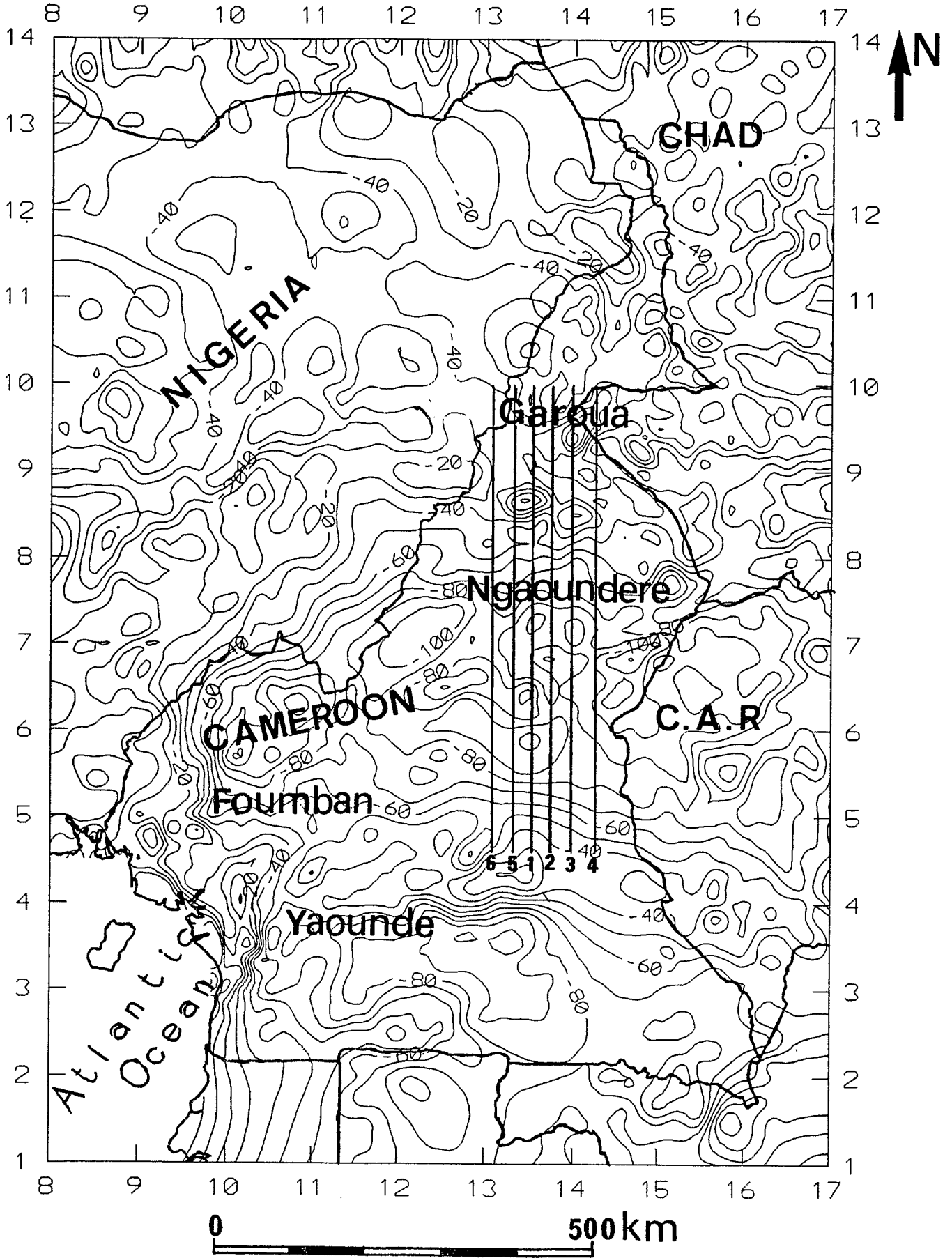


Fig. 3. Bouguer anomaly map of Cameroon (Collignon, 1968) and location of the six profiles used in this study. Note the long wavelength Bouguer anomaly on the Adamawa massif.

- Using seismic refraction data and teleseismic delay times, Dorbath and Dorbath (1984) studied the structure of the crust and upper mantle beneath the Adamawa uplift. They found an abnormally thin crust (23 km) underlain by an upper mantle with anomalously low P-wave velocity (7.8 km.s^{-1}) for the northern margin of the uplift. The southern part is characterized by a crust with a normal thickness (33 km) and a normal upper mantle P-wave velocity (8.0 km.s^{-1}). According to these results, the lithosphere is revealed as thin in the northern part of Adamawa where the rocks are essentially volcanic.

COHERENCE FUNCTION ANALYSIS

The method

Our aim is to study the mechanical behaviour of the lithosphere beneath the Adamawa uplift by determining its effective elastic thickness (EET). Model interpretations of the coherence function in terms of the flexural rigidity of the lithosphere commonly assume that the lithosphere is deformed by the application of surface loads (McKenzie and Bowin, 1976; Banks *et al.*, 1977; McNutt and Parker, 1978; Loudon and Forsyth, 1982; McNutt, 1983).

Forsyth (1985) studied the importance of surface and subsurface loading on the determination of the flexural rigidity of the lithosphere for continental regions. He showed that the coherence function is, as compared to the admittance function (Lewis and Dorman, 1970; McNutt and Parker, 1978), the best way to quantify the flexural rigidity of the lithosphere in continental areas, since the interpretation of the admittance function leads to underestimates of the effective elastic thickness of the lithosphere (see Forsyth, 1985; Cochran, 1980), in the presence of sub-surface loads. This approach has been later on widely used in continental areas and proved to be efficient. Moreover, several results were obtained in Africa: Banks and Swain (1978); Bechtel *et al.* (1987) for the Kenya dome; Lesquer *et al.* (1988) for the Hoggar massif; Jallouli (1989) for the Air massif; Bonvalot (1990) for Fouta-Djalon (see Fig. 1 for location of these features).

The coherence function quantifies the relationship of the topography and the Bouguer anomaly in a given area as a function of wave number. Its shape is controlled by the rigidity of the plate:

- If the plate is weak ($T_e \rightarrow 0$), a load from below produces a topographic dome and a surface load creates a compensation root. The coherence is thus close to 1. This feature corresponds to the classical Airy model.

- If the plate is rigid ($T_e \rightarrow \infty$), there is no compensation of the surface and (or) subsurface

loads. Therefore, topography and gravity are not correlated and thus the coherence is close to 0.

- Finally, if the plate has a non zero rigidity ($T_e > 0$), loads are compensated at long wavelengths (coherence close to 1) and uncompensated at short wavelengths (coherence close to 0). The wavelength of the transition from compensated to uncompensated topography provides a direct estimation of the flexural rigidity and thus of the effective elastic thickness, since the flexural rigidity and the EET (T_e) are related by:

$$D = \frac{E T_e^3}{12 (1-\nu^2)} \quad (1)$$

where E is the Young's modulus = 10^{11} Nm^{-1} , ν denotes the Poisson's ratio = 0.25

To compute the coherence, it is possible to use either a 2d or a 3d approach according to the structure to be studied. In our case, since the Adamawa is an elongated feature, we used a 2d approach.

An estimation of the coherence is given by the following formula (e. g. Bendat et Piersol, 1986):

$$Co(k) = \frac{\langle B(k) G^*(k) \rangle \langle B^*(k).G(k) \rangle}{\langle B(k).B^*(k) \rangle \langle G(k).G^*(k) \rangle} \quad (2)$$

where $B(k)$ and $G(k)$ are the Fourier transform for topography and gravity respectively.

* is the complex conjugate sign and the angle brackets denote the averaging in the spectral domain over a series of profiles.

Munk and Cartwright (1966) showed that this estimation of the coherence could be affected by noise in the data sets. So they suggested to compute the coherence using the formula:

$$C(k) = \frac{n Co(k) - 1}{n - 1} \quad (3)$$

where n is the number of profiles and $Co(k)$ is the coherence defined by equation (2)

We also estimated the error on each value of coherence using the following equation (Bendat and Piersol, 1986):

$$E_{coch} = \frac{|1 - C(k)| \sqrt{2 * |C(k)|}}{\sqrt{n}} \quad (4)$$

The data

The data used in this study were acquired by several surveys carried out by ORSTOM (France)

in Cameroon between 1960 and 1967. From these data, we computed six profiles oriented N-S and running perpendicular to the Adamawa trend (Fig. 3). The locations of the profiles were chosen such that they are as close as possible to the original data. For each point of a profile, Bouguer anomaly and topography values were obtained by interpolation applying a least square method of all the original points contained in a given radius of 20 km around the computed point. Each profile is 600 km long and the sampling interval is equal to 6 km.

Figure 4 shows the six resulting profiles. This figure reveals that there is generally a good negative correlation between gravity and topography. This correlation was also pointed out by Okereke (1984). For example, the mean Bouguer gravity is close to -100 mgals (200 km wide) over the Adamawa plateau where the average topography is nearly 1000 metres above mean sea level.

We computed the Fourier transform of the data using an algorithm which does not require a number of points as a power of two. Two treatments were checked to minimize the edge effect:

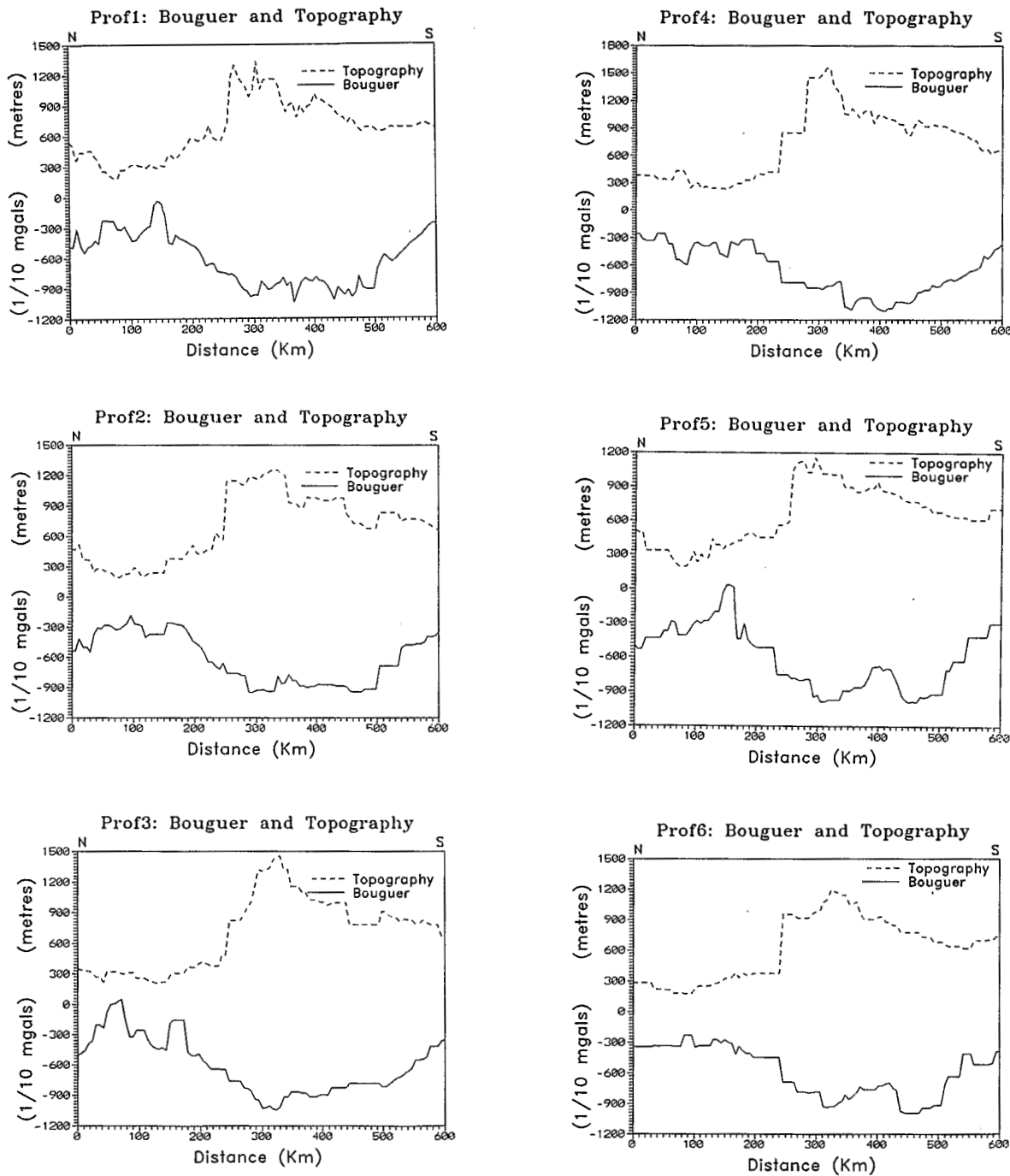


Fig. 4. Plot of the six profiles with the topography and the Bouguer anomaly.

mirror imaging and derivative (Diament, 1985). Due to the finite length of the data in the spatial domain, the coherence function that is computed in the frequency domain has a sampling interval given by $1/1$ and is theoretically defined up to the Nyquist frequency ($N/21$) with 1 is the length of the profile and N the number of points. The transition from one to zero for the coherence function lies at 100 to 200 km. Therefore, it is controlled by very few points especially since the estimation of the coherence function at short wavelength is biased by noise. Thus, to get significant information of the experimental coherence function, we varied the length of the profiles from 320 to 600 km taking care that the Adamawa massif was well centered. This treatment allows us to get better results than the usual approach does. Figure 5 shows the computed coherence for the six profiles and for several lengths.

RESULTS AND INTERPRETATION

Both treatments of the edge effect give similar results. As predicted, three main wavebands can be distinguished:

- the long wavelength domain ($l > 300$ km); the coherence is very close to 1.0
- the short wavelength band ($l < 100$ km) where the coherence approaches 0.0
- the wavelength of the transition from coherent to incoherent topography and gravity occurs in the same range as the transition from compensated to uncompensated topography ($100 < l < 300$ km). This wavelength of the transition is well controlled due to the numerous estimations of the coherence obtained by varying the length of the profiles.

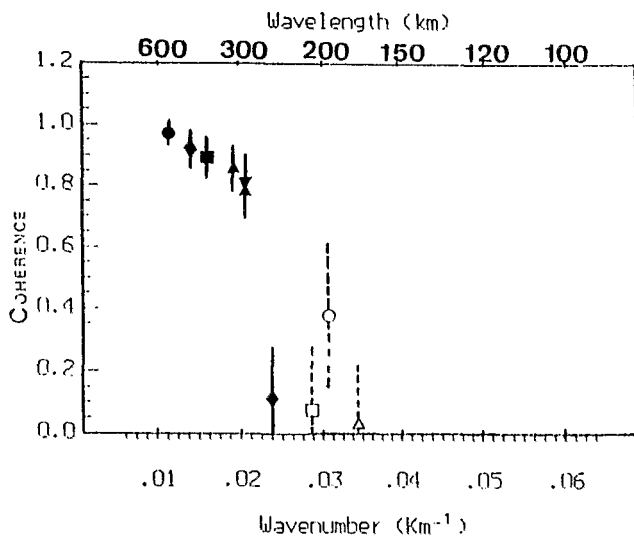


Fig. 5. Observed coherence for the Adamawa region versus the wavenumber. The empty symbols indicate the points obtained with a large error band. The edge effects here were avoided by a mirror imaging treatment (coherence: ● at 600 km length, ◆ at 480 km, ■ at 430 km, ▲ at 360 km, and ✕ at 320 km).

The observed coherence was fitted to some predicted coherence curves with different elastic thicknesses and load ratio values (subsurface versus surface load) to find the elastic thickness of the lithosphere for Adamawa region. The best fit is obtained for an Effective Elastic Thickness of 20 km and a load ratio $f = 0.8$. The flexural rigidity is thus of about $0.7 \cdot 10^{23}$ Nm (Fig. 6).

It is known that the Effective Elastic Thickness of a lithosphere increases with increasing plate age. Since continents are on average very old, the thermal effect is not so apparent as that of oceanic plates (e. g. Watts *et al.*, 1980), and the elastic plate thickness is caused by massive failure in the lower continental crust. Nevertheless, the values of the Effective Elastic Thickness in continental areas generally vary from 25 to more than 100 km (see McNutt *et al.*, 1988). But for domal uplifts and continental rift areas, the Effective Elastic Thickness is lower and close to 30 km. The Effective Elastic Thickness obtained in this study for the Adamawa region lies in the range of values found for thermal domes (see Table 1). On the other hand, some preliminary studies were carried out on this uplifted area. Indeed, Girod (1984) analysed some mantle rocks from volcanic pipes in south Adamawa. He found that the rocks were essentially made of peridotite and plagioclase developed in temperature and pressure conditions that correspond to less than 25 km depth. We can recall that Le Marechal (1970) studied some thermal phenomena beneath the Adamawa uplift.

The value of the load ratio ($f = 0.8$) means that the subsurface load, produced by abnormal mantle beneath the Adamawa region, is slightly less than the topographic load. This is probably due to volcanism. To better constrain the depth of the low density zone, inferred from interpretation of the long wavelength Bouguer gravity anomaly by

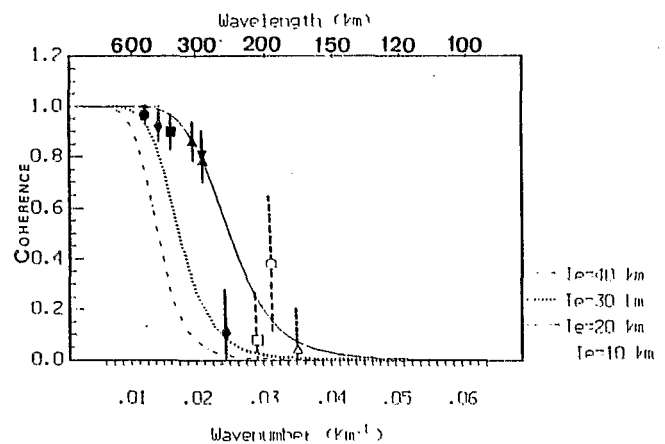


Fig. 6. Fit of the observed coherence (the symbols) with some predicted coherence curves (Forsyth, 1985). The numbers denote different values of Effective Elastic Thickness. The best fit is obtained for an EET equal to 20 km and thus a flexural rigidity of about $0.7 \cdot 10^{23}$ Nm.

Table 1. Effective Elastic Thicknesses for some rifts and domes.

Name of the region	Effective elastic thickness (km)	Reference
DARFUR DOME	43	Ebinger <i>et al.</i> , 1989
FOUTA DJALON	20 - 50	Bonvalot (1990)
HOGGAR MASSIF	35	Lesquer <i>et al.</i> , 1988
ADAMAWA MASSIF	20	The present study
AIR MASSIF	20 - 30	Jallouli (1989)
KENYA RIFT	21 - 36	Ebinger <i>et al.</i> , 1989
BAIKAL RIFT	30	Diamant <i>et al.</i> , 1989

Browne and Fairhead (1983), we performed a spectral analysis of our profiles.

SPECTRAL ANALYSIS AND SOURCE-DEPTH ESTIMATION

To estimate the depth to the major density contrasts within the lithosphere of the Adamawa plateau, we applied spectral analyses to Bouguer gravity data. This method has been widely used by several authors (e. g. Spector and Grant, 1970; Pal, Khuruna and Unnikrishvan, 1979).

Spector and Grant (1970) showed that if $S(t)$ is a series of N samples with a constant step interval Δt , the discrete Fourier transform of this series is given by:

$$S(k) = 1/N \sum_{t=0}^N S(t) \cdot \exp(-2\pi kt/N) \quad (6)$$

$$k = 0, \dots, N-1$$

The power spectrum is thus:

$$E(k) = |S(k)|^2 \quad (7)$$

The fft algorithm is normally used for infinite record processing. For finite length series as it is the case here, the periodic extension of the signal exhibits discontinuities at the boundaries of the observation. These discontinuities are responsible for spectral leakage as it was the case for the coherence function analysis. To suppress the leakage problem, it is common practice, to window the data, and so reduce the order of the discontinuities on the edge of the records to be analyzed. For this purpose, several windows are proposed by Harris (1978). The power spectrum shows frequency intervals where the logarithms of the amplitudes may be represented by a linear function of frequency. The slope of the straight line is proportion-

al to the depth to the top of the body.

To estimate the source depth from this power spectrum, we used the approach proposed by K. Dimitriadis *et al.* (1987). After the logarithm of the power spectrum is plotted versus the wave number, the depth is estimated using a linear regression method. For each window, we selected the proper linear segments; the depth to the source for the specific window and the corresponding rms error is evaluated. This error is estimated according to the points which define the segments chosen.

We used the same six profiles as for the coherence function analysis. To solve the leakage problem, we applied three windows on the profiles: Hanning, Blackman-Harris and the Kaiser-Bessel windows and we also used a mirror imaging treatment. We chose these windows because they are characterized by a highly concentrated central lobe and a very low sidelobe structure (Harris, 1978).

Fig. 7 shows, for one of the six profiles, the plot of the logarithm of the power spectrum versus the wave number, using the four treatments. Each plot can be approximated by three main straight line segments. And we can estimate the source depth using the slopes of those segments. Table 2 lists, for each window and for each profile, the depth to the source and the corresponding rms error. It should be noted that for some treatments (e.g., mirror imaging), the second segment and the corresponding source depth are not resolved.

Table 2 shows that the source depth estimations using the four treatments are within a few km. To select the most reliable values, we checked the windows with synthetic data by constructing a gravity model with a body at a given depth. We thus computed the corresponding gravity anomaly produced by this body, and, using this anomaly, we computed the source depths for the four treatments. The method which provided the best result, identical to the synthetic model, was the Kaiser-Bessel window. Therefore, we selected the source depths obtained with this window, as shown on Fig. 8 for profiles 3 and 4.

- The first line on the figures dominates the low wave numbers ($k < 0.02 \text{ km}^{-1}$) and the calculated depth (h_1) is of about 70 to 90 km.

- The second segment dominates the mid-wave numbers ($0.02 < k < 0.06$) with a depth (h_2) in the range of 18 to 38 km.

- Finally, the third straight line occupies the high wave numbers ($k > 0.06$) and the corresponding depth (h_3) is between 4 and 15 km.

These values of the depth source are of the same order as those obtained by Fairhead and Okereke (1988) using a grid of gravity data on the Adamawa region. The calculated depths are in good agree-

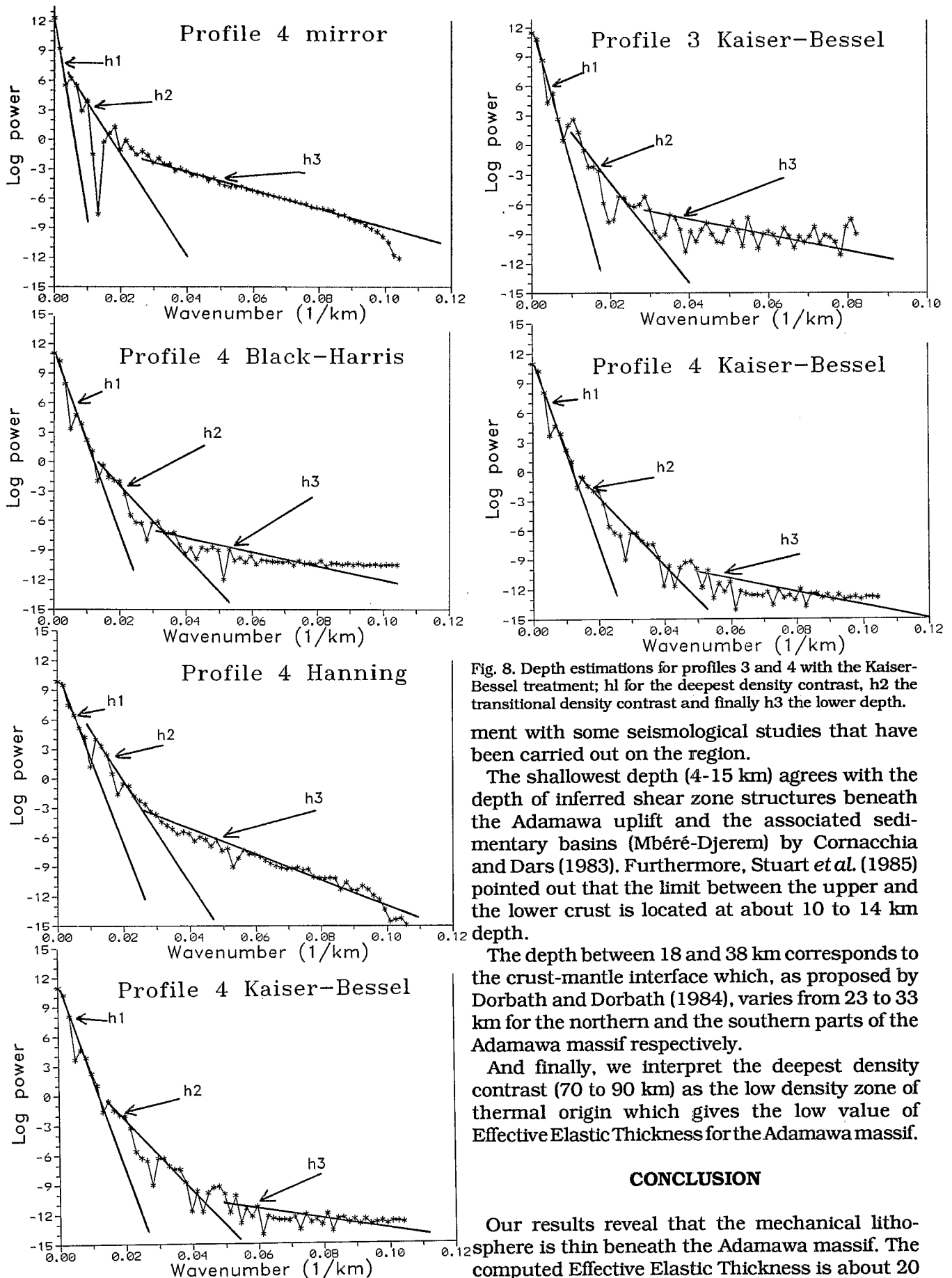


Fig. 7. Plot of the power spectrum versus the wavenumber for profile 4 and different treatments.

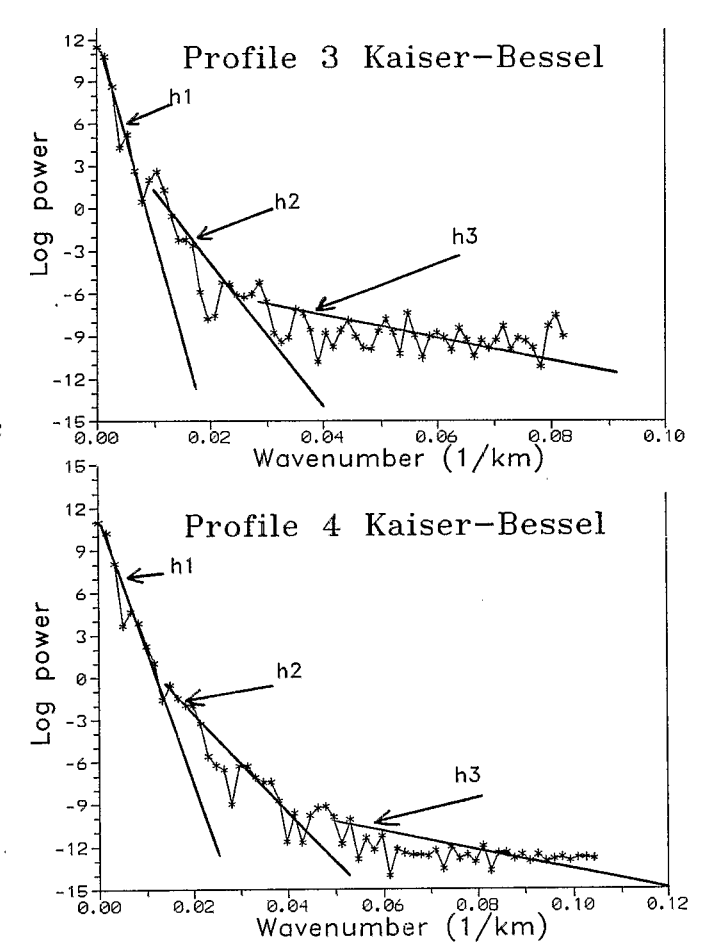


Fig. 8. Depth estimations for profiles 3 and 4 with the Kaiser-Bessel treatment; h1 for the deepest density contrast, h2 the transitional density contrast and finally h3 the lower depth.

ment with some seismological studies that have been carried out on the region.

The shallowest depth (4-15 km) agrees with the depth of inferred shear zone structures beneath the Adamawa uplift and the associated sedimentary basins (Mbéré-Djerem) by Cornacchia and Dars (1983). Furthermore, Stuart *et al.* (1985) pointed out that the limit between the upper and the lower crust is located at about 10 to 14 km depth.

The depth between 18 and 38 km corresponds to the crust-mantle interface which, as proposed by Dorbath and Dorbath (1984), varies from 23 to 33 km for the northern and the southern parts of the Adamawa massif respectively.

And finally, we interpret the deepest density contrast (70 to 90 km) as the low density zone of thermal origin which gives the low value of Effective Elastic Thickness for the Adamawa massif.

CONCLUSION

Our results reveal that the mechanical lithosphere is thin beneath the Adamawa massif. The computed Effective Elastic Thickness is about 20 km. This value of the EET is of the same order of magnitude as those obtained for the other African

Table 2. Source depth estimations (km) for the six profiles and for different treatments

	Mirror imaging	Hanning window	Black-Harris window	Kaiser-Bessel window
Profil 1	h1 = 64 ± 0.8 h2 = undet. h3 = 7 ± 0.6	h1 = 66 ± 1.8 h2 = 17 ± 0.5 h3 = 5 ± 0.2	h1 = 56 ± 1.6 h2 = undet. h3 = 6.5 ± 0.3	h1 = 85 ± 6.4 h2 = 38 ± 1.0 h3 = 4 ± 0.1
Profil 2	h1 = 87 ± 4.5 h2 = undet. h3 = 12 ± 0.2	h1 = 68 ± 2.0 h2 = 17 ± 0.8 h3 = 10 ± 0.3	h1 = 71 ± 3.0 h2 = undet. h3 = 9 ± 1.6	h1 = 74 ± 6.0 h2 = 34.8 ± 0.6 h3 = 6 ± 0.3
Profil 3	h1 = 90 ± 2.6 h2 = undet. h3 = 6 ± 0.5	h1 = 66 ± 2.5 h2 = 32 ± 0.3 h3 = 5 ± 0.1	h1 = 82 ± 1.7 h2 = 43 ± 0.7 h3 = 4 ± 0.6	h1 = 78 ± 6.5 h2 = 33 ± 0.8 h3 = 4 ± 0.6
Profil 4	h1 = 82 ± 7.1 h2 = 36 ± 5.2 h3 = 7 ± 0.1	h1 = 62 ± 1.8 h2 = 31 ± 0.3 h3 = 8 ± 0.6	h1 = 71 ± 3.1 h2 = 43 ± 0.7 h3 = 9 ± 0.6	h1 = 70 ± 2.7 h2 = 27 ± 0.6 h3 = 7 ± 0.6
Profil 5	h1 = 50 ± 1.4 h2 = undet. h3 = 7 ± 0.1	h1 = 50 ± 3.8 h2 = 30 ± 1.3 h3 = 10 ± 0.1	h1 = 77 ± 1.3 h2 = undet. h3 = 4.5 ± 0.3	h1 = 79 ± 1.3 h2 = undet. h3 = 15 ± 0.6
Profil 6	h1 = 44 ± 6 h2 = 20 ± 0.4 h3 = 4 ± 0.1	h1 = 78 ± 2.4 h2 = 26 ± 0.5 h3 = 8 ± 0.2	h1 = 71 ± 1.3 h2 = 45 ± 1.0 h3 = 4 ± 0.6	h1 = 76 ± 1.8 h2 = 25 ± 0.4 h3 = 9 ± 0.2

uplifts (Air, Hoggar, Darfur, Fouta-Djalou) and some continental rift areas (Kenya, Baikal). Thus, this favours the idea that the African uplifts were formed by similar processes.

The spectral analysis allows us to locate three major density contrasts. These depth estimations are in good agreement with seismological studies. The shallowest depth (4-15 km) agrees with the seismic limit of the upper and lower crust (10-14 km) as proposed by Stuart *et al.* (1985). The second density contrast (18-36 km) corresponds to the Moho (Dorbath and Dorbath, 1984). Finally, the 70 to 90 km depth is interpreted as the depth of a zone of partial melting producing the volcanic activity beneath the Adamawa massif. This depth corresponds to the top of the upper mantle that was proposed by C. and L. Dorbath (1984) to be abnormal.

Acknowledgements - We thank C. Ebinger and R. Black for many fruitful discussions on the text.

REFERENCES

- Almeida, F. M. et Black, R. 1967. Comparaison structurale entre le Nord-est du Brésil et l'Ouest Africain. Symp. Continental Drift, Montevideo.
- Banks, R. J., Parker R. L. and Huestis, S. P. 1977. Isostatic compensation on a continental scale: local versus regional mechanisms. *Geophys. J. R. Astron. Soc.* **51**, 431-452.
- Banks, J. and Swain, C. 1978. The isostatic compensation of East Africa. *Proc. R. Astron. Soc. Ser. A* **364**, 331-352.
- Bechtel, T. D. D., Forsyth, D. W. and Swain, C. 1987. Mechanism of isostatic compensation in the vicinity of the East African rift, Kenya. *Geophys. J. R. Astron. Soc.* **90**, 445-465.
- Bendat, S., Piersol, A. G. 1986. Random data: analysis and measurement procedures, second edition, Wiley ed., 566 p.
- Bonvalot, S., 1990. Mesures gravimétriques en Guinée et Sierra-Leone, Modélisation structurale et étude du comportement mécanique de la lithosphère: étude d'une chaîne péricratonique, d'un bombement intra-plaque et de marges transformantes. *Thèse Université Paris VI*.
- Browne, S. E. and Fairhead, J. D. 1983. Gravity study of the Central African rift system: a model of continental disruption. 1. The Ngoundere and Abu Gabra rifts. *Tectonophysics* **94**, 187-203.
- Cochran, J. R. 1980. Some remarks on isostasy and the long-term behavior of the continental lithosphere. *Earth Planet. Sci. Letters.* **46**, 266-274.
- Cornacchia, M. et Dars, R. 1983. Un trait structural majeur du continent africain. Les linéaments centrafricains du Cameroun au Golfe d'Aden. *Bull. Soc. Géol. Fr.* **25**, 101-109.
- Diament, M. 1985. Influence of method of data analysis on admittance computation. *Annales Geophysicae* **3/6**, 785-792.

- Diament, M. and Kogan, M. G. 1990. Long wavelength gravity anomalies and the deep thermal structure of the Baikal rift. *Geophys. Res. Letters* **17/11**, 1977-1980.
- Dimitriadis, K., Tselentis, G. A. and Thanassoulas, K. 1987. A basic program for 2-D spectral analysis of gravity data and source depth estimation. *Computers and Geosciences* **13/5**, 549-460.
- Dorbath, L., Dorbath, C., Stuart, G. W. et Fairhead, J. D. 1984. Structure de la croûte sous le plateau de l'Adamaoua (Cameroun). *C. R. Acad. Sc. Paris* **298**, Ser. II, 539-542.
- Duncan, R. A. 1981. Hot spot in the southern oceans, an absolute frame of references for motions of the Gondwana continent. *Tectonophysics* **74**, 29-42.
- Ebinger, C. J., Bechtel, T. D., Forsyth, D. W. and Bowin, C. O. 1989. Effective Elastic Plate Thickness beneath the East African and Afar plateaus and dynamic compensation of the uplifts. *J. Geophys. Res.* **94**, N°B3, 2883-2901.
- Fairhead, D. and Okereke, C. S. 1988. Depths to major density contrasts beneath the West-African rift system in Nigeria and Cameroon based on the spectral analysis of gravity data. *Journal of African Earth Sciences* **7**, 5/6, 769-777.
- Fitton, G. 1980. The Benue trough and Cameroon volcanic line - a migrating rift system in West Africa. *Earth and Planetary Science Letters* **51**, 132-138.
- Fitton, G. 1983. Active versus passive continental rifting: evidence from the West-African rift system. *Tectonophysics* **94**, 473-481.
- Forsyth, D. W. 1985. Subsurface loading and estimate of flexural rigidity of continental lithosphere. *J. Geophys. Res.* **90**, N°B14, 12623-12632.
- Harris, F. J. 1978. On the use of windows for the harmonic analysis with discrete Fourier transform. *Proceedings of the IEEE* **66/1**.
- Jallouli, C. 1989. Caractérisation du comportement mécanique de la lithosphère continentale à partir de données gravimétriques; implications géodynamiques pour la chaîne pan-africaine du Sahara Central de l'Afrique (Air). Thèse de Doctorat Université de Paris Sud, Orsay.
- Le Marechal, A. 1976. Géologie et géochimie des sources thermominérales du Cameroun. Trav. Doc. ORSTOM, 59.
- Lesquer, A., Bourmatte, A. and Dautria, 1988. Deep structure of the Hoggar domal uplift (Central Sahara, South Algeria) from gravity, thermal and petrological data. *Tectonophysics* **152**, 71-87.
- Lewis, B. T. R. and Dorman, L. M. 1970. Experimental isostasy, 2. An isostatic model for the USA derived from gravity and topography data. *J. Geophys. Res.* **75**, 3367-3386.
- Louden, K. E. and Forsyth, D. W. 1982. Crustal structure and isostatic compensation near the Kane fracture zone from topography and gravity measurements, 1, Spectral analysis approach. *Geophys. J. R. Astron. Soc.* **68**, 725-750.
- Louis, P. 1970. Contribution géophysique à la connaissance du bassin du Lac Tchad. *Mém. ORSTOM* **42**, 311.
- Louis, P. 1978. Gravimétrie et géologie en Afrique occidentale et Centrale. *Mém. B.R.G.M.* **91**, 53-61.
- Masclé, P. 1976. Le Golfe de Guinée (Atlantique Sud): un exemple d'évolution de marges atlantiques en cisaillement. *Mém. Soc. Géol. France* **128**, 104.
- Mc Kenzie, D. P. and Bowin, C. 1980. The relationship between bathymetry and gravity in the Atlantic Ocean. *J. Geophys. Res.* **85**, 6377-6396.
- Mc Nutt, M. K. 1983. Influence of plate subduction on isostatic compensation in northern California. *Tectonophysics* **2**, 399-415.
- McNutt, M. K. and Parker, R. L. 1978. Isostasy in Australia and the evolution of the compensation mechanism. *Science* **199**, 773-775.
- Munk, W. and Cartwright, D. E. 1966. Tidal spectroscopy and prediction. *Philos. Trans. R. Soc. London* **259**, 553-589.
- Pal, P. C., Khuruna, K. K. and Unnikrishnan, P. 1979. Two examples of the spectral approach to source depth estimation in gravity and magnetics. *Pageoph* **117** (78/79), Birgauser Verlag, Basel.
- Reyre, D. 1984. Remarques sur l'origine et l'évolution des bassins sédimentaires africains de la côte atlantique. *Bull. Soc. Géol. Fr.* **26/6**, 1041-1059.
- Spector, A. and Grant, F. S. 1970. Statistical models for interpreting aeromagnetic data. *Geophysics* **35**, 293-302.
- Stuart, G. W., Fairhead, J. D., Dorbath, L. and Dorbath, C. 1985. A seismic refraction study of the crustal structure associated with the Adamawa Plateau and Garoua rift, Cameroon, West Africa. *Geophys. J. R. Astron. Soc.* **81**, 1-12.
- Tchoua, F. 1974. Contribution à l'étude géologique et pétrographique de quelques volcans de la ligne du Cameroun (Monts Manengouba et Bambouto). *Thèse Univ. Clermont-Ferrand*, 347.
- Vincent, P. M. 1970. The evolution of the Tibesti volcanic province, eastern Sahara. In: *African magmatism and tectonics*, (edited by T. M. Clifford and I. G. Gass), 301-309. Oliver and Boyd edition, Edinburgh.